

# Comparison of Compressive Creep Characteristics of Commercial Zinc-Based Alloys No3 and No5

A. A. Mir

University Centre Leeds, UK

Park Lane, Hanover Lane, Leeds LS3 1AA, UK

Research was carried out at Aston University, Aston Triangle, Birmingham B4 7ET, UK

---

## Abstract

Creep tests are commonly performed by applying constant stress or load to uniaxial specimens, and creep data is obtained in the form of creep strain versus test time. This creep data is further used to determine creep related parameters, such as primary creep extension, the secondary creep rate, time to 1 % creep strain or stress to fracture at a given time.

Compressive creep tests have been carried out on two commercial zinc-rich alloys No3 and No5. These tests were performed on a standard weighted lever arm constant load compressive creep machine using hollow cylindrical test pieces. The nominal stress range for these tests was 20 to 100 MPa at temperatures from 70 to 160°C.

Generally, the primary creep extension was found to increase with copper content and was therefore higher in alloy No5, but the secondary creep rates of No5 were much lower than those of No3. Similarly, time to 1 % creep strain was greater for No5. It was concluded from these tests that alloy No5 had a total creep deformation significantly lower than No3 under all testing conditions due to its lower secondary creep rates and thus had better compressive creep strength than alloy No3.

**Keywords:** Compressive Creep, Commercial Zinc-based Alloys, Primary Creep, Secondary Creep Rates, Creep Strength

---

Date of Submission: 04-02-2025

Date of Acceptance: 16-02-2025

---

## I. INTRODUCTION

The commercial zinc-based alloys No3 and No5 were the first major commercial zinc alloys developed. These alloys are widely used as useful engineering materials especially in automotive industry [1] for many decades. They have a good combination of mechanical and physical properties particularly relatively low melting temperatures, excellent ability in casting and especially their ability to be cast in the highest speed die-casting machines, long term dimensional stability, fluidity characteristics, lower material cost and lower density [2,3,4]. These attributes make them successful competitors against other non-ferrous alloys since their introduction.

It is an important design requirement to determine the compressive and tensile creep of materials used in commercial applications, particularly at moderately elevated temperatures. Research has been carried out to determine the tensile creep strength of these alloys in the past [5, 6, 7, 8] but so far no attempt has been made to investigate their compressive creep behaviour. Since compressive creep is important in many zinc alloys applications, especially when they are used in automotive where compression is common, it was therefore imperative to study and compare the compressive creep properties of these alloys in detail.

### COMPRESSIVE CREEP MACHINE

The machine was designed for compressive creep testing of different materials. Most of the fabrication and machining work of machine has been accomplished in the Manufacturing and Production Laboratory of Aston University. The machine is of the standard lever loading type with a lever arm ratio of 10:1. The machine has the following main parts:

1. Three vertical supporting columns with a lever which is placed on the top of these columns
2. A hydraulic-jack which plays an important role in the smooth application of load on the specimen. Initially the hydraulic-jack sustains the applied load, and then transfers it to the specimen very smoothly at the start of the experiment
3. An oil-bath which is used to heat the specimen up to the required constant temperature and maintain it until the

termination of the test. The operating temperature of the oil-bath is 45 to 300°C and the extended temperature range with additional cooling of -100 to 300°C. The temperature controller has an accuracy of 0.01-0.03°C.

4. The strain recording equipment consists of a transducer, strain indicating instrument and the computer. The values of creep deformation are shown according to the time intervals selected in the measurement and control software called 'Windmill'. This software was purchased so that creep strain can be recorded precisely. The 'Windmill' programme has been modified according to the creep testing requirements. For this purpose, at the start of the test, the time interval between two readings of creep strain is very small, i.e. five seconds which are increased gradually and eventually the last time interval is one hour.

The computer shows the creep data in the form of time (s) versus strain (mm).

## II. EXPERIMENTAL WORK

The specimens used for creep testing were prepared from sand castings of alloys. These specimens were of cylindrical shape, having the following finished dimensions: length = 30 mm, diameter = 13 mm, bore (plain) = 8 mm.

The alloys used in sand castings were taken from stock materials with guaranteed compositions. The test pieces for all creep experiments were fabricated and machined on a lathe in the Manufacturing and Production Laboratory of Aston University. During the production of the test samples, the machining operation was carefully controlled so as to reduce variations in surface finish to a minimum.

**Compressive creep testing:** The specimens were loaded axially in compression and dipped into the oil-bath which was set at the required test temperature. Before the start of the experiment, a reasonably long time was allowed for the temperature of oil-bath and test sample to stabilise. The temperature changes of the specimen were kept to a maximum of 0.5°C for the whole period of the test. The temperature of the specimen inside the oil-bath was measured by a digital potentiometer, using chromel/alumel thermocouples which were attached to the specimen, to check for, and thus avoid, any temperature gradients along the gauge length of the specimen.

The resulting creep deformation was recorded in the form of creep strain versus time by the strain recording equipment and displayed by the computer through the "Windmill" measurement and control software, which was designed particularly for these types of tests.

Various stresses from 20 to 100 MPa and temperatures from 70 to 160°C were used during these tests. The experiments were conducted to a minimum creep contraction of 1%.

## III. RESULTS OF CREEP TESTS

Curves of creep strain (%) versus time (s) were obtained for various combinations of applied stress and testing temperature. Examples of these creep curves have been shown in Figs. 1 and 2 for alloys No3 and No5, respectively. From these curves, the primary creep, secondary creep rate and times to achieve total creep strains of 0.5, 0.7 and 1% were also obtained.

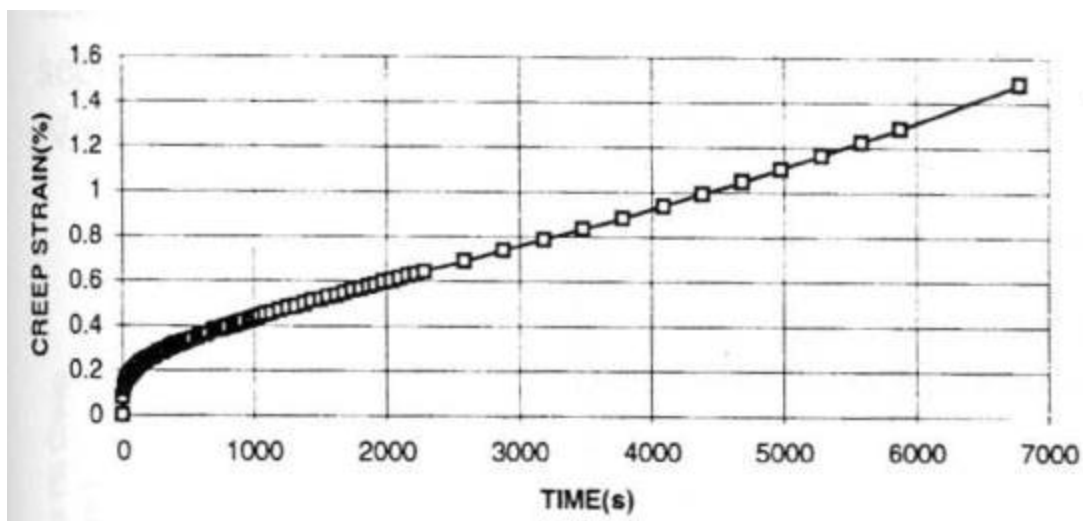


Figure 1: Creep curve of alloy NO3 at 60 Mpa and 130 °C

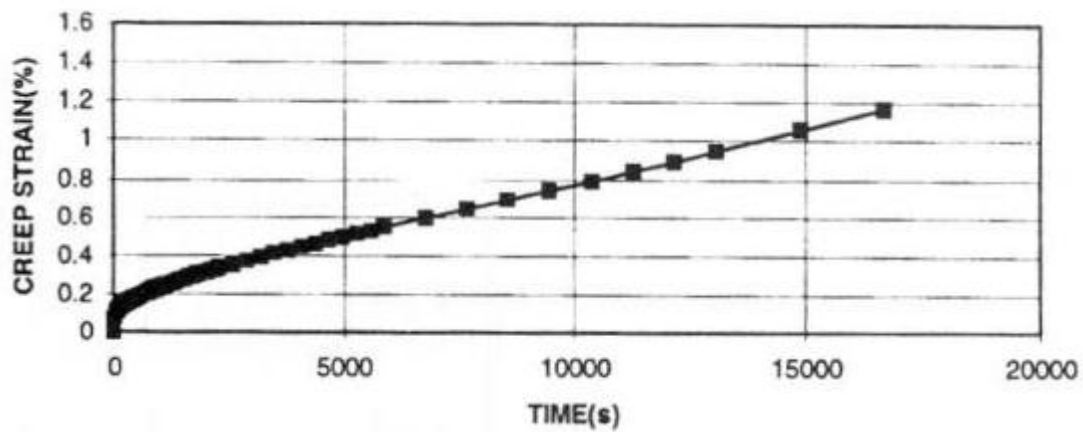


Figure 2: Creep curve of alloy NO5 at 40 MPa and 160 °C.

**Primary creep contraction:** Primary creep is defined as the creep deformation obtained by extrapolating the linear secondary creep portion of the creep curve back to zero time. For both alloys, the values of the primary creep (%) were calculated from creep curve of each test. No clear dependence of the primary creep on the testing conditions was observed, but the average values of primary creep for both alloys were generally found to increase with decreasing temperature. The average values of primary creep for each alloy were also found to vary with the copper content. The data showed that it increased with increasing copper content and therefore the average values for alloy No5 were greater than those for No3. The average primary creep contractions versus copper content have been shown in Fig. 3 for both alloys.

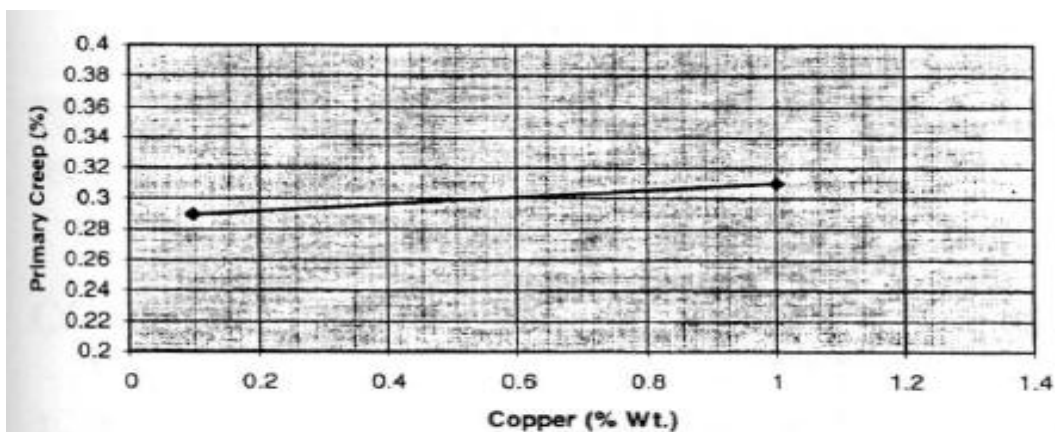


Figure 3: Variation primary creep with copper content of alloys NO3 and NO5.

**Secondary creep rate:** Secondary creep rate is the average rate of strain in the linear portion of the creep curve which follows the primary stage. Secondary creep rate has been measured for each test for both alloys and the results plotted in the form of  $\ln$  secondary creep rate versus  $\ln$  stress are shown in Figs. 4 and 5. These plots showed a reasonably good correlation with constant slopes for both alloys over much of the stress and temperature range, although deviations were observed at low stresses and low temperatures for both alloys.

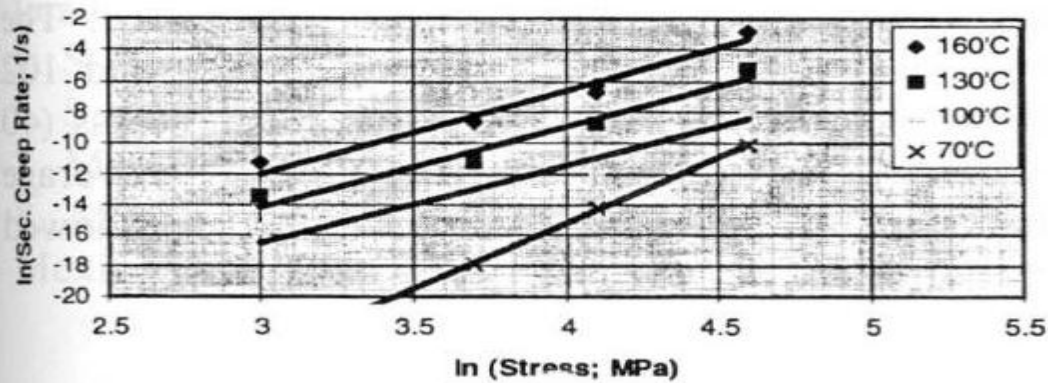


Figure 4: Variation of secondary creep rates with applied stress at different temperatures for alloy NO3.

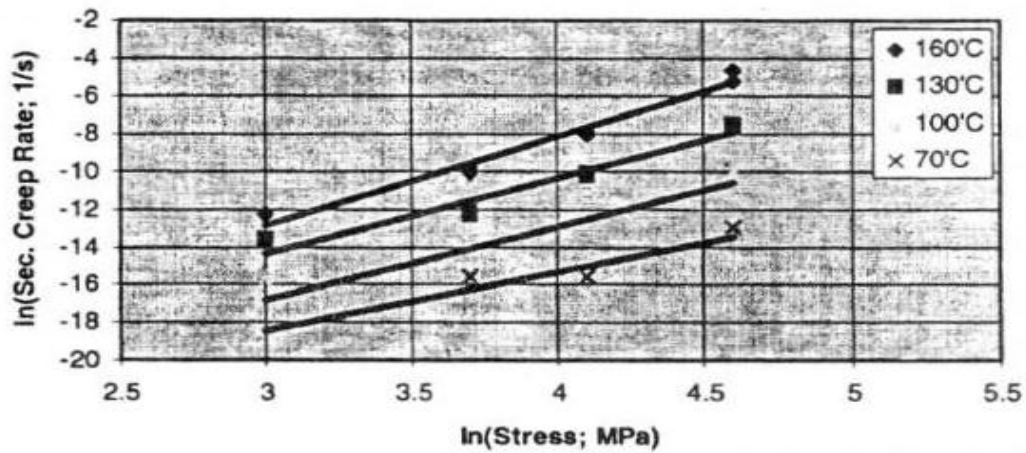


Figure 5: Variation of secondary creep rates with applied stress at different temperatures for alloy NO5.

The average values of slopes (stress exponent) for alloys No3 and No5 were found to be 5.1 and 4.2, respectively. The secondary creep rates (1/s) obtained at different stresses (40 to 100 MPa) are listed in Tables 1 to 3 for the temperature range of 100 to 160°C for both alloys.

Table 1 - Secondary creep rates (1/s) of alloys at 100 MPa.

Temp. (°C)	100	130	160
No3	$4.21 \times 10^{-4}$	$5.07 \times 10^{-3}$	$6.04 \times 10^{-2}$
No5	$4.03 \times 10^{-5}$	$5.38 \times 10^{-4}$	$5.30 \times 10^{-3}$



Table 2 - Secondary creep rates (I/s) of alloys at 60 MPa.

Temp. (°C)	100	130	160
No3	$1.21 \times 10^{-5}$	$1.63 \times 10^{-4}$	$1.91 \times 10^{-3}$
No5	$2.13 \times 10^{-6}$	$3.72 \times 10^{-5}$	$3.28 \times 10^{-4}$

Table 3 - Secondary creep rates (I/s) of alloys at 40 MPa.

Temp. (°C)	100	130	160
No3	$1.38 \times 10^{-6}$	$1.93 \times 10^{-5}$	$1.89 \times 10^{-4}$
No5	$3.47 \times 10^{-7}$	$4.68 \times 10^{-6}$	$4.41 \times 10^{-5}$

**Total creep contraction:** For both alloys, the times to a total creep contraction of 0.5, 0.7 and 1% were obtained from the creep curves. At different stresses, the log times to 1 % creep strain for both alloys were then plotted as a function of the reciprocal of the testing temperature (K), and shown in Fig. 6. It was observed that these plots were linear with a constant slope (Q/R) over much of the stress range. The average values of the activation energy (Q) for alloys No3 and No5 were calculated as 103 and 102 kJ/mole, respectively. However, deviations from this slope appeared for both alloys at lower stress (40 MPa) and the lowest test temperature of 70°C. The overall creep performances of the alloys as average values of times(s) to produce 1% creep strain can be compared from Table 4. This comparison showed that total creep performance of alloy No5 was much better than No3.

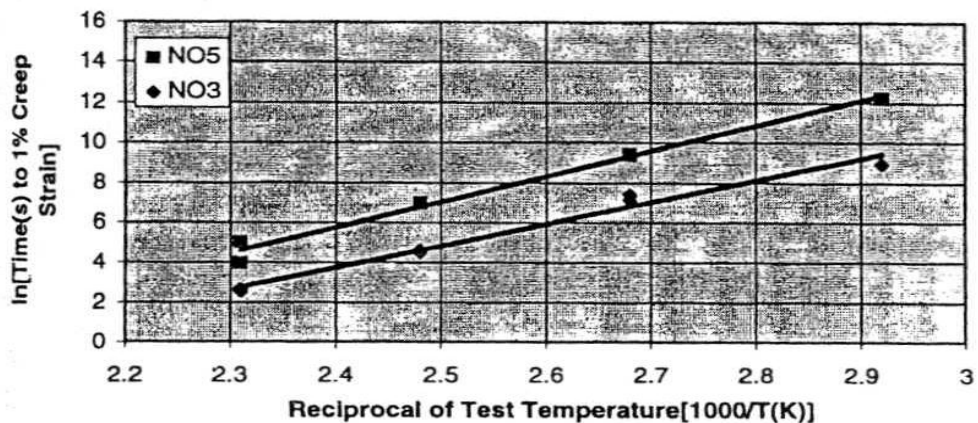


Figure 6: ln time to 1% creep strain vs reciprocal of test temperature at 100MPa.

Table 4 – Average values of times (s) to produce 1% creep strain at 100 MPa

Temp. (°C)	100	130	160
NO3	1425	96	14
NO5	11890	1040	77

**METALLOGRAPHY OF THE EXPERIMENTAL ALLOYS**

Scanning electron microscopy (SEM) in back-scattered electron imaging mode was used as the general investigation method to study the microstructure of these commercial alloys. The contrast in the electron microscope images depends almost entirely on the average atomic number of different phases present in the structure of the alloys. Therefore in the SEM micrographs of these alloys, zinc-rich phases appeared light and aluminium-rich phases dark, since zinc-rich phase had more electron scattering power due to its higher atomic number and produced a greater number of back-scattered electrons than that of the aluminium-rich phase with lower atomic number although the shade of contrast could be adjusted by varying electronically the sensitivity of the electron detector to the atomic number.

**Alloy No3**

The as-cast structure of alloy No3 is shown in Figs. 7 and 8 at two different appropriate magnifications. The figures showed that the structure of the alloy was very heterogeneous and hypoeutectic, consisting of a few large and numerous small primary zinc-rich ( $\eta$ ) dendrites. These dendritic particles were surrounded by a relatively small volume of lamellar eutectic matrix. The whole structure was fine due to the grain refinement produced by the addition of magnesium. It was also observed that many small rounded dark particles of the Al-rich former  $\beta$  phase were attached to the primary  $\eta$  phase dendrites. The development of these dark, Al-rich particles on the primary zinc-rich  $\eta$  is shown at higher magnification in Fig. 8. It was clear from this figure that this phase was the Al-rich eutectic  $\beta$  phase which had nucleated on the primary phase ( $\eta$ ) at high undercooling during eutectic solidification.  $\beta$  phase is unstable below about the eutectoid temperature of 275°C and decomposes into Zn-rich  $\eta$  and Al-rich  $\alpha$  phases. Fig. 8 indicates that the  $\beta$  in both the particles and the  $\beta$  constituent of the lamellar matrix had decomposed. In addition, the edges of the primary  $\eta$  dendrites were decorated with small Al-rich particles.

The structure of the alloy No3 after being creep-tested in compression at 100 MPa and 160°C is shown in Figs. 9 and 10. Due to short duration of the test, great changes in the structure of alloy were not expected. However, the primary  $\eta$  dendrites had much larger volume than the eutectic, similar to that observed for the as-cast structure. The figures showed no significant change in the size of primary particles. The lamellae of eutectic matrix were well-developed (Fig. 9), and were generally smaller than those in the as-cast structure. Small precipitates within the primary particles were observed in both as-cast and creep-tested conditions.



**Figure 7:** As cast structure (SEM) of Alloy No3 at medium magnification (350x) showing former  $\beta$  attached to primary  $\eta$  dendrites

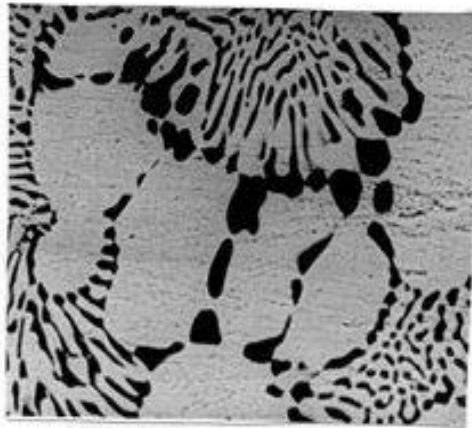


**Figure 8:** As cast structure (SEM) of AlloyNo3 at high magnification (645x)

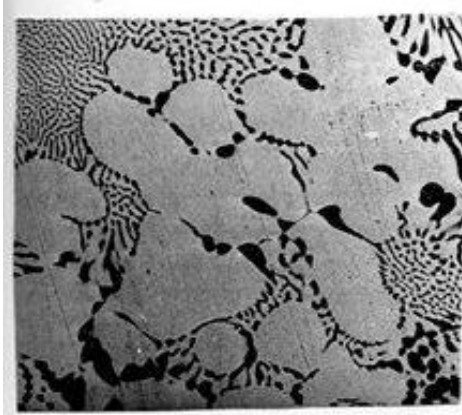


**Figure 9:** SEM. AlloyNo3 tested at 100 MPa and 160°C at medium magnification (356x)

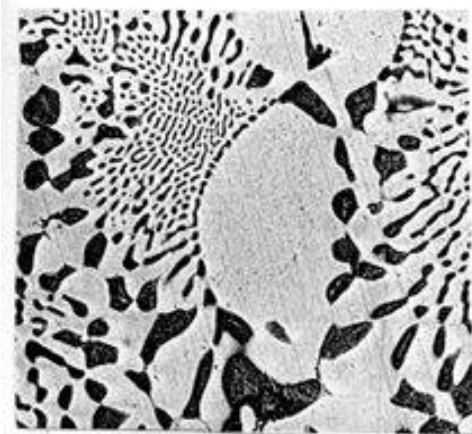


**Figure 10:** SEM micrograph of Alloy No3 tested at 100 MPa and 160°C at high magnification (655x)

### **Alloy No5**

The as-cast structure of alloy No5 is shown in Figs. 11 and 12 at medium and high magnifications, respectively. The scale of the structure was similar to that of alloy No3 with more uniformly distributed primary Zn-rich ( $\eta$ ) particles. Like alloy No3, the structure of this alloy also consisted of large and small primary Zn-rich dendrites surrounded by lamellar eutectic matrix. The main difference from the structure of alloy No3 was that the size of primary particles in this case was larger as compared to those of No3, also the primary  $\eta$  dendrites and the  $\eta$  component of the ( $\alpha + \eta$ ) eutectic had copper-rich  $\epsilon$ -phase precipitates. It was difficult to differentiate these precipitates from zinc ( $\eta$ ) particles due to a very small difference in atomic numbers of both zinc and copper. The volume of eutectic matrix was relatively small as compared to primary particles. Many small and dark particles of Al-rich former  $\beta$  phase were observed which were attached to the

hypoeutectic  $\eta$  particles (similar to No3). These are shown at higher magnification in Fig. 11.  $\beta$  is unstable below the eutectoid temperature of 275°C and transforms into Zn-rich  $\eta$  and Al-rich  $\alpha$  phases.

Figs. 13 and 14 show the structure of alloy No5 after compressive creep testing at 20 MPa and 160°C which represents the alloy structure at the lowest applied stress and the highest test temperature. The volume of eutectic matrix was slightly reduced as compared to the as-cast structure. The micrographs also showed the regular eutectic ( $\alpha+\eta$ ) morphology, and it was believed that the higher creep resistance of alloy No5 was due to this regular morphology combined with the strong strengthening effect of the  $\epsilon$ -phase precipitates.

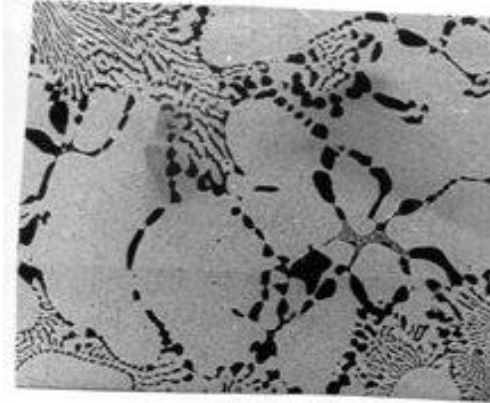


**Figure 11:** As cast structure (SEM) of Alloy No5 at medium magnification (308x) showing primary  $\eta$  particles with relatively small volume of eutectic

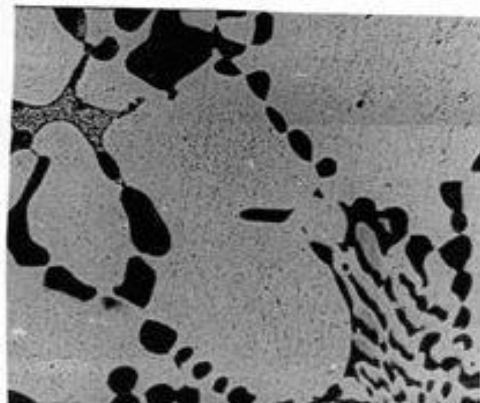


**Figure 12:** SEM. As cast structure of Alloy No5 at high magnification (618x) showing primary  $\eta$  particles with Al-rich  $\beta$  phase and eutectic

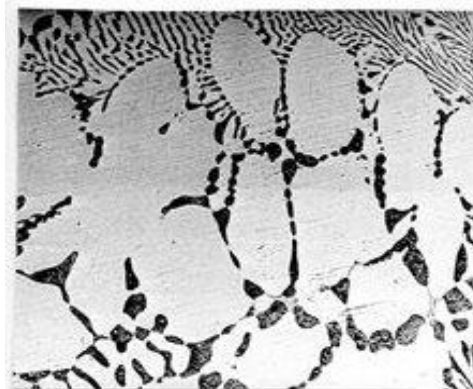


**Figure 13:** SEM. Alloy No5 tested at 20 MPa and 160°C at medium magnification (363x) showing dark particles of Al-rich  $\beta$  phase



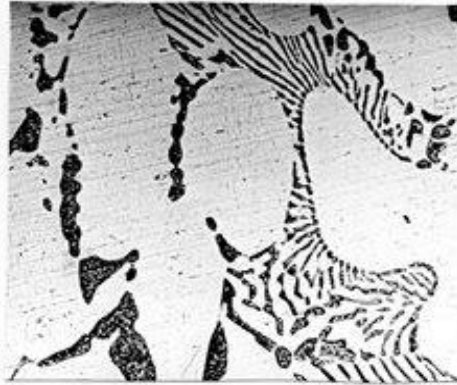


**Figure 14:** SEM micrograph of Alloy No5 tested at 20 MPa and 160°C at high magnification (668x)

#### IV. DISCUSSION

From the creep test data of both alloys, it was found that in general alloy No3 had smaller primary creep strain than No5. The mean values of primary creep for alloys No3 and No5 were found to be 0.29 and 0.31%, respectively. These values showed that there was not much difference in the primary creep of both alloys.

The composition of alloy No3 shows that it consists mainly of zinc with a small amount of aluminium and some impurities. It therefore has the least complex microstructure consisting largely of zinc-rich primary  $\eta$  dendrites surrounded by a relatively small volume of lamellar eutectic matrix of  $\alpha$  and  $\eta$ , after cooling to room temperature.

The comparison of creep results of alloy No3 with those of alloy No5 showed that No3 had significantly higher creep rate than No5 under all testing conditions. At higher temperatures, No3 had much lower overall creep resistance than alloys No5 and No2 (by a factor of about 2-40). It has already been proved [9] that the creep strength of the primary  $\eta$  particles in No3 is lower than that of the eutectic, therefore the lower overall creep resistance of this alloy is mainly due to the primary  $\eta$  particles having comparatively greater volume than eutectic in the microstructure.

The solid solubility of aluminium (in equilibrium) in zinc is 1.1% at 382°C (eutectic temperature) and decreases to a very small value at room temperature whereas the excess aluminium is removed by precipitation of aluminium as a phase ( $\alpha$ ) in zinc-rich matrix upon solidification.

According to previous research on tensile creep of Zn-Al alloys[9], the creep strength of a pressure die-cast zinc-based alloy with no aluminium was higher than that of alloy No3, and it was concluded that the creep resistance of zinc was further reduced by the precipitation of aluminium as a phase in the zinc matrix. This trend has also been observed in zinc alloys with small amounts of aluminium (0.2 and 0.4 %). It has been reported [9] that these alloys had better super plasticity than a series of binary Zn-Al alloys including the Zn-Al eutectoid alloy at low temperatures, but they did not exhibit super plasticity at a high temperature of 250°C. This behaviour was expected since in low Al-Zn alloys, all the aluminium dissolved in the zinc solid solution at 250°C because the solubility of aluminium in zinc is 0.42% at 227°C [10]. However, sand-cast alloy No3 showed a better overall creep performance in compression (current research) than the pressure die-cast alloy without aluminium previously investigated [9] for tensile creep. In the case of sand-cast alloy, the matrix of zinc is weak and has low creep resistance whereas the eutectic of  $\alpha$  plates has a good lamellar structure and should provide a high resistance to creep.

Since total creep deformation is considered very important design parameter for most creep environments, it is therefore evident that No5 showed a considerably better creep resistance than No3 due to its much lower secondary creep rates. High creep strength of alloy No5 was due to its higher copper content (1 %) than No3 which contained only about 0.03 weight% of copper.

#### V. CONCLUSIONS

1. Alloy No5 had higher primary creep than No3 which meant that primary creep increased with an increase of copper content
2. Alloy No5 had much lower values of secondary creep rates as compared to alloy No3.
3. Using the time to a total creep deformation of 1 % as a measure, alloy No5 was found to have much better creep resistance than No3
4. Due to short duration of the test, great changes in the structure of alloys were not expected.

However, in alloy No3 the primary  $\eta$  dendrites had much larger volume than the eutectic, like that observed for the as-cast structure. There were no significant changes in the size of primary particles. The lamellae of eutectic

matrix were well-developed, and were generally smaller than those in the as-cast structure. Small precipitates within the primary particles were observed in both as-cast and creep-tested conditions

5. The microstructure of alloy No5 shows that the volume of eutectic matrix was slightly reduced as compared to the as-cast structure. The micrographs also showed the regular eutectic ( $\alpha+\eta$ ) morphology, and it was believed that the higher creep resistance of alloy No5 was due to this regular morphology combined with the strong strengthening effect of the  $\varepsilon$ -phase precipitates

6. Higher compressive creep strength of alloy No5 was due to increased copper content (1%) which had a profound effect in increasing the creep resistance of this alloy

#### REFERENCES

- [1]. Mathewson C H, Zinc-The Science and Technology of the Metal, Its Alloys and Compounds. Reinhold Publishing Corporation, New York, 1959
- [2]. Apelian D, Paliwal M, Herrschaft D C, JOM, 33 (1981) 12-20
- [3]. Technical Notes on Zinc-Zinc alloy die castings, Zinc Development Association, London, 1983
- [4]. Goodwin FE, Ponikvar AL, Eds. Engineering Properties of Zinc Alloys, 3rd edn.- revised, Int. Lead Zinc Research Organization Inc, USA, 3-8, 1989
- [5]. Murphy S, Savaskan T and Hill J, Can. Metall. Quarterly, 25 (1986) 145-150
- [6]. Murphy S, Durman M, Hill J, Z. Metallkunde, 79 (1988) 243-247
- [7]. Durman M, Murphy S, Z. Metallkunde, 82 (1991) 129-134
- [8]. Durman M, Murphy S, in Advances in Science, Technology and Applications of Zn-Al
- [9]. Alloys, edited by Villasenor GT, Zhu Y H, Pina C (Mexico), 1994
- [10]. Durman M, The Creep Behaviour of Pressure Die Cast Zinc-Aluminium Based Alloys. PhD Thesis, Aston University, Birmingham, UK, 1989
- [11]. Mondolfo L F, Aluminium Alloys – Structure and Properties. Butterworth, London, 1976